

Electronic Supplementary Material (ESI) for Dalton Transactions.

This journal is © The Royal Society of Chemistry 2018

Supporting Information

Extremely stable europium-organic framework for luminescent sensing $\text{Cr}_2\text{O}_7^{2-}$ and Fe^{3+} in aqueous system

Yan-Li Gai,^a Qin Guo,^a Xue-Yan Zhao,^a Yan Chen,^a Shan Liu,^a Yuan Zhang,^a Chun-
Xue Zhuo,^a Cui Yao,^a and Ke-Cai Xiong^{*a}

^a School of Chemistry and Materials Science, Jiangsu Normal University, Xuzhou, Jiangsu
221116, P.R. China

● Corresponding author:

* E-mail: kcxiang@jsnu.edu.cn.

Contents

1. Experiment section
2. Table S1. Crystallographic data for Ln-MOFs.
3. Table S2. Comparison of sensing ability of Eu-MOFs.
4. Figure S1. The topology architecture of Eu-MOF.
5. Figure S2. The PXRD and TGA diagrams of Ln-MOFs.
6. Figure S3. Solid luminescent spectra of Ln-MOFs excited based on ligand absorption.
7. Figure S4. The PXRD patterns of Eu-MOF before and after immersing in $\text{Cr}_2\text{O}_7^{2-}$ aqueous solution for 5 hours and 24 hours.
8. Figure S5. The PXRD patterns of Eu-MOF before and after immersing in Fe^{3+} aqueous solution for 5 hours and 24 hours.
9. Figure S6. The IR diagrams of Eu-MOF before and after immersing in $\text{Cr}_2\text{O}_7^{2-}$ aqueous solution for 5 hours and 24 hours.
10. Figure S7. The IR diagrams of Eu-MOF before and after immersing in Fe^{3+} aqueous solution for 5 hours and 24 hours.
11. Figure S8. The UV-vis absorption spectra of different cations (0.15 mM) in water solution.
12. Figure S9. The UV-vis absorption spectra of different anions (0.15 mM) in water solution.

EXPERIMENT SECTION

Instruments

The purity of the bulk samples were determined by Bruker D8 Advance powder X-ray diffractometer. Thermal stability were performed on TA Q50 apparatus in the temperature range of 30-800 °C under nitrogen atmosphere. Elemental analyses (C, H and N) were performed on an Elementar Vario MICRO elemental analyzer. The infrared spectra were recorded on a Thermo Scientific Nicolet iS10 FT-IR spectrometer as KBr pellets in the range of 400-4000 cm^{-1} . The UV-Vis absorption spectra were recorded on a Thermo Scientific NanoDrop 2000c spectrometer. The solid state emission and excitation spectra were tested on a Horiba Jobin-Yvon Fluorolog-3 spectrophotometer. Luminescent behavior in aqueous solution were recorded on Agilent Cary Eclipse.

Structure determination

Data collection for Ln-MOFs were performed on Bruker APEXII diffractometer equipped with graphite monochromated Mo- $K\alpha$ radiation ($\lambda = 0.71073 \text{ \AA}$) by using the ω -scan and ϕ -scan mode at room temperature. The structures were solved by direct methods followed by successive difference Fourier methods, and refined on F^2 by full-matrix least-squares using SHELXTL-2018 program package. All non-hydrogen atoms were refined anisotropically. Ligand 1,3-bdc²⁻ that generated by the operation of inversion center was disordered, and hydrogen atoms on it were not determined. The other hydrogen atoms of organic ligands were generated theoretically. The number of lattice water molecules was determined according to the results of the thermogravimetry and elemental analysis. The molecular formulas for all Ln-MOFs contain the lattice water molecules that were not determined according to difference Fourier peaks. Crystallographic data of Ln-MOFs were listed in Table S1.

Syntheses

H₂LCl₂ was synthesized according to the method reported.^[1] Other reagents in analytical grade were commercially purchased from Aladdin and Sinopharm and used without further purification.

[Eu₂L(1,3-bdc)₃]·5H₂O: 0.01 mmol (42 mg) H₂LCl₂, 0.02 mmol (32 mg) 1,3-H₂bdc, 0.01 mmol (35 mg) Eu₂O₃ were added to the 20 mL Telfon-lined stainless steel container, following with 6 mL deionized H₂O. Then the mixture was heated at 140 °C for 96 hours. After cooling to room temperature, colorless crystals were obtained with further filtration. Anal. Calcd. for C₄₄H₃₈Eu₂N₂O₂₁ (%): C, 42.80; H, 3.10; N, 2.27. Found (%): C, 42.73; H, 3.16; N, 2.20. IR (KBr, cm⁻¹): 3423 (s), 3034 (w), 1652(s), 1607(s), 1450 (s), 1397 (s), 1181 (w), 1133 (w), 1078 (w), 917 (w), 844 (m), 784 (w).

[Sm₂L(1,3-bdc)₃]·5H₂O: The synthesized procedure was same with Eu-MOF except lanthanide salt. 0.01 mmol (35 mg) Sm₂O₃ was used instead of Eu₂O₃. Anal. Calcd. for C₄₄H₃₈Sm₂N₂O₂₁ (%): C, 42.29; H, 3.23; N, 2.24. Found (%): C, 42.25; H, 3.08; N, 2.38. IR (KBr, cm⁻¹): 3431 (s), 3034 (w), 1651 (s), 1607 (s), 1547 (s), 1480 (s), 1449 (s), 1398 (s), 1181 (w), 1133 (w), 1078 (w), 917 (w), 844 (w), 743 (w).

[Dy₂L(1,3-bdc)₂]·5H₂O: The method was same with Eu-MOF but using 0.01 mmol (37 mg) Dy₂O₃ instead of Eu₂O₃. Anal. Calcd. for C₄₄H₃₈Dy₂N₂O₂₁ (%): C, 41.49; H, 3.17; N, 2.20. Found (%): C, 42.17; H, 3.16; N, 2.29. IR (KBr, cm⁻¹): 3435 (s), 3034 (w), 1659 (s), 1608 (s), 1551 (s), 1454 (s), 1401 (s), 1183 (w), 1160 (w), 1133 (w), 1079 (w), 1044 (w), 1021 (w), 920 (w), 847 (m), 744 (s).

Table S1 Crystallographic data for Ln-MOFs.

Compounds	Eu-MOF	Sm-MOF	Dy-MOF
Crystal system	Triclinic	Triclinic	Triclinic
Space group	<i>P</i> -1	<i>P</i> -1	<i>P</i> -1
<i>a</i> (Å)	10.0810(8)	10.0830(7)	10.0735(12)
<i>b</i> (Å)	11.4845(9)	11.4747(8)	11.4617(14)
<i>c</i> (Å)	12.2758(10)	12.2880(9)	12.2530(14)
α (°)	117.1100(10)	117.1020(10)	117.1650(10)
β (°)	99.5530(10)	99.4780(10)	99.5150(10)
γ (°)	104.7060(10)	104.6280(10)	104.7310(10)
<i>V</i> (Å ³)	1156.32(16)	1158.21(14)	1150.4(2)
<i>Z</i>	2	2	2
<i>T</i> (K)	296(2)	296(2)	296(2)
Measured reflections	6863	8236	6933
Independent reflections	5032	5102	5051
<i>R</i> _{int}	0.0144	0.0164	0.0144
<i>D</i> _c (g cm ⁻³)	1.661	1.654	1.700
<i>F</i> (000)	564	562	562
<i>S</i>	1.082	1.169	1.048
<i>R</i> ₁ (<i>I</i> > 2σ(<i>I</i>)) ^a	0.0355	0.0347	0.0399
<i>wR</i> ₂ (<i>I</i> > 2σ(<i>I</i>)) ^b	0.0989	0.0949	0.1083

$$^a R_1 = \frac{\sum ||F_o| - |F_c||}{\sum |F_o|}, \quad ^b wR_2 = \frac{[\sum w(F_o^2 - F_c^2)^2 / \sum w(F_o^2)^2]^{1/2}}{\sum w(F_o^2)^2}$$

Table S2. Comparison of sensing ability in terms of quenching coefficient (*K*_{sv}) and detection limitation (DL) of Eu-MOFs towards Cr₂O₇²⁻ and Fe³⁺.

Compounds	Medium	Analytes	Quenching coefficient (<i>K</i> _{sv} , M ⁻¹)	Detection limitation (DL, M)	Refs
[Eu ₂ L(1,3-bdc) ₃]·5H ₂ O	H ₂ O	Cr ₂ O ₇ ²⁻	1.55 × 10 ⁴	^a 9.2 × 10 ⁻⁶	This work
		Fe ³⁺	1.25 × 10 ⁴	^a 2.3 × 10 ⁻³	
[Eu(HL)(H ₂ O) ₂ (NO ₃)]·NO ₃	H ₂ O	Cr ₂ O ₇ ²⁻	7.52 × 10 ⁴	^a 1.7 × 10 ⁻⁵	S1
		Fe ³⁺	4.03 × 10 ⁴	^a 4.3 × 10 ⁻⁵	
[EuL(Himdc)(ina)(H ₂ O)]	H ₂ O	Cr ₂ O ₇ ²⁻	2.46 × 10 ³	^b 10 ⁻⁵	S2
		Fe ³⁺	1.30 × 10 ⁴	^b 10 ⁻⁵	
[Eu(HL)(H ₂ O) ₃]	H ₂ O	Cr ₂ O ₇ ²⁻	5.50 × 10 ³	^a 5.1 × 10 ⁻⁴	S3
		Fe ³⁺	5.30 × 10 ³	^a 1.2 × 10 ⁻³	
[Eu(L) ₂ (NO ₃) ₂]	CH ₃ CN	Cr ₂ O ₇ ²⁻	1.06 × 10 ⁴	^b 10 ⁻⁶	S4
		Fe ³⁺	1.39 × 10 ⁴	^b 10 ⁻⁷	
[Eu(ppda)(bdc) _{0.5} (C ₂ H ₅ OH)(H ₂ O)]	DMF	Cr ₂ O ₇ ²⁻	4.03 × 10 ³	^b 10 ⁻⁵	S5
		Fe ³⁺	2.10 × 10 ⁴	^b 10 ⁻⁵	
[Eu ₂ (L) _{1.5} (H ₂ O) ₂ (EtOH)]·	DMF	Cr ₂ O ₇ ²⁻	1.53 × 10 ³	^b 10 ⁻⁵	S6

DMF		Fe ³⁺	2.94 × 10 ³	^b 10 ⁻⁵	
[Eu ₃ (L) ₂ (OH) (DMF) _{0.22} (H ₂ O) _{5.78}]	DMF	Cr ₂ O ₇ ²⁻	6.63 × 10 ³	—	S7
		Fe ³⁺	—	^a 1.8 × 10 ⁻⁵	
[Eu(Hpzbc) ₂ (NO ₃) ₂ ·H ₂ O]	EtOH	Cr ₂ O ₇ ²⁻	—	^a 2.2 × 10 ⁻⁵	S8
		Fe ³⁺	2.6 × 10 ³	^a 2.6 × 10 ⁻⁵	
Eu-BDC-NH ₂	DMF	Cr ₂ O ₇ ²⁻	7.32 × 10 ³	—	S9
		Fe ³⁺	4.93 × 10 ³	—	
Eu-BDC-F	DMF	Cr ₂ O ₇ ²⁻	9.69 × 10 ³	—	
		Fe ³⁺	7.52 × 10 ³	—	
Eu-1,4-NDC	DMF	Cr ₂ O ₇ ²⁻	1.12 × 10 ⁴	—	
		Fe ³⁺	9.34 × 10 ³	—	

^a Detection limitation calculated by $3\delta/k$; ^b Detection limitation according to the experiment data which is usually much lower than the calculated value since the error exists in calculation.

[Eu₂L(1,3-bdc)₃]·5H₂O, H₂LCl₂: 4-Bis(4-carboxylatopyridinium-1-methylene)benzene dichloride

[Eu(HL)(H₂O)₂(NO₃)₂]·NO₃, H₂L: 4-(3,5-dicarboxylphenyl)-2-methylpyridine

[EuL(H₂O)₂]·NMP·H₂O, H₃L: 4,4',4''-striazine-1,3,5-triyltri-m-aminobenzoate

[EuL(Himdc)(ina)(H₂O)], H₃imdc: imidazole-4,5-dicarboxylic acid; Hina: isonicotinic acid

[Eu(HL)(H₂O)₃], H₄L: 1-(3,5-dicarboxylatobenzyl)-3,5-pyrazole dicarboxylic acid

[Eu(L)₂(NO₃)₂], H₂L: 3-bis(3-carboxyphenyl)imidazolium

[Eu(ppda)(bdc)_{0.5}(C₂H₅OH)(H₂O)], H₂ppda: 4-(pyridin-3-yloxy)-phthalic acid

[Eu₂(L)_{1.5}(H₂O)₂(EtOH)]·DMF, H₄L: 5,5'-(carbonylbis(azanediyl))diisophthalic acid

[Eu₃(L)₂(OH)(DMF)_{0.22}(H₂O)_{5.78}], H₄L: 3,5-bis(isophthalic acid)-1H-1,2,4-triazole

[Eu(Hpzbc)₂(NO₃)₂]·H₂O, H₂pzbc: 3-(1H-pyrazol-3-yl) benzoic acid

References

- S1. W. Gao, F. Liu, B.-Y. Zhang, X. M. Zhang, J.-P. Liu, E. Q. Gao and Q. Y. Gao, *Dalton Trans.*, 2017, **46**, 13878.
- S2. L. H. Liu, X. T. Qiu, Y. J. Wang, Q. Shi, Y. Q. Sun and Y. P. Chen, *Dalton Trans.*, 2017, **46**, 12106.
- S3. W. Q. Tong, T. T. Liu, G. P. Li, J. Y. Liang, L. Hou and Y. Y. Wang, *New J. Chem.*, 2018, **42**, 9221.
- S4. Y. Yang, F. Qiu, C. Xu, Y. Feng, G. Zhang and W. Liu, *Dalton Trans.*, 2018, **47**, 7480.
- S5. X. Zhang, Z. Zhan, X. Liang, C. Chen, X. Liu, Y. Jia and M. Hu, *Dalton Trans.*,

2018, **47**, 3272.

S6. W. Liu, X. Huang, C. Xu, C. Chen, L. Yang, W. Dou, W. Chen, H. Yang and W. Liu, *Chem. Eur. J.*, 2016, **22**, 18769.

S7. J. Q. Liu, G. P. Li, W. C. Liu, Q. L. Li, B. H. Li, R. W. Gable, L. Hou and S. R. Batten, *Chempluschem*, 2016, **81**, 1299.

S8. G. P. Li, G. Liu, Y. Z. Li, L. Hou, Y. Y. Wang and Z. Zhu, *Inorg. Chem.*, 2016, **55**, 3952.

S9. P. Yi, H. Huang, Y. Peng, D. Liu and C. Zhong, *RSC Adv.*, 2016, **6**, 111934.

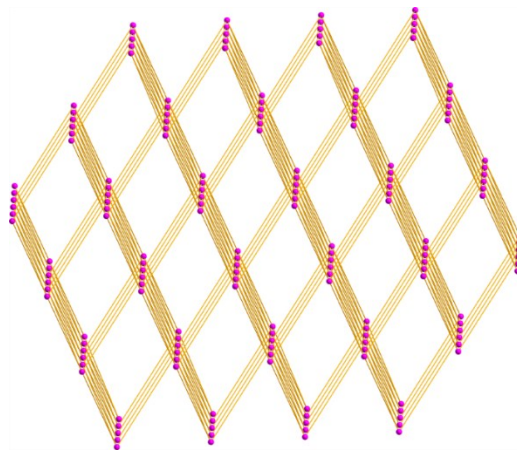


Figure S1. The topology architecture simplified by means of six-connected nodes (Eu^{3+} paddlewheel dinuclear) and two-connected linkers (ligands L and $1,3\text{-bdc}^{2-}$).

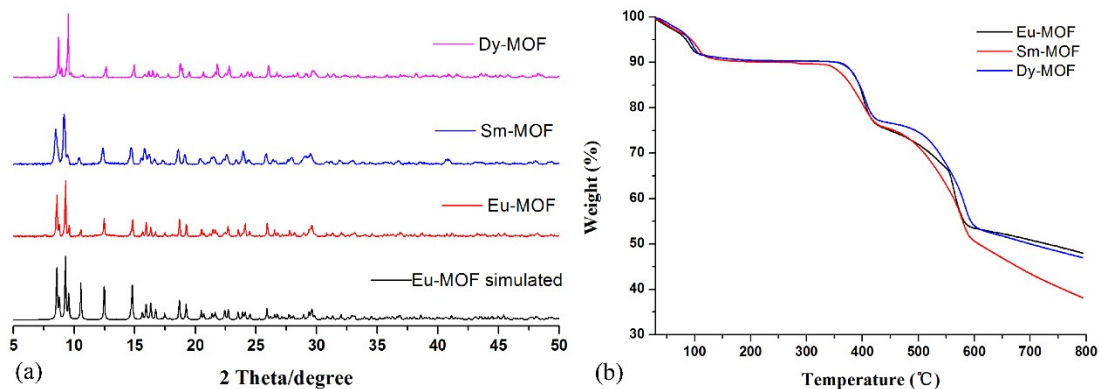


Figure S2. (a) The PXRD patterns of Ln-MOFs; (b) The TGA diagrams of Ln-MOFs.

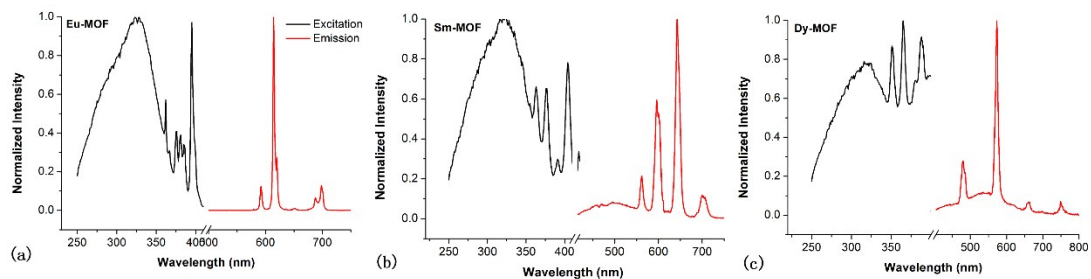


Figure S3. Solid luminescent spectra of Ln-MOFs excited based on ligand absorption.

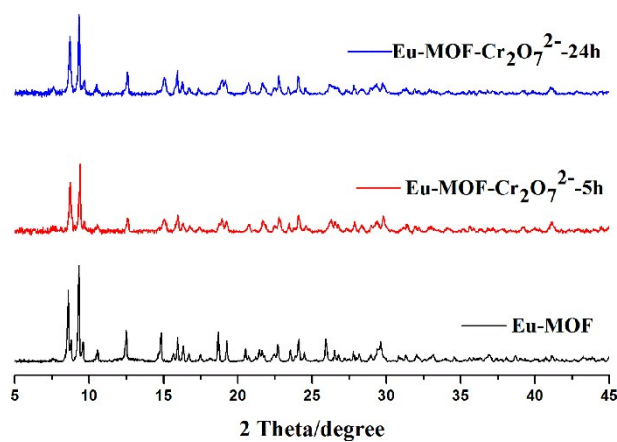


Figure S4. The PXRD patterns of Eu-MOF before and after immersing in Cr₂O₇²⁻ aqueous solution for 5 hours and 24 hours.

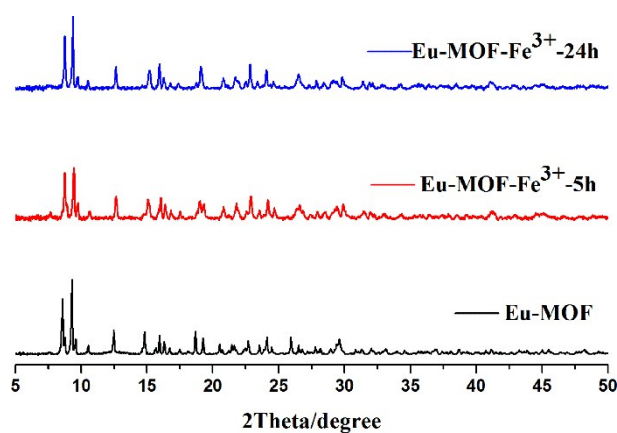


Figure S5. The PXRD patterns of Eu-MOF before and after immersing in Fe³⁺ aqueous solution for 5 hours and 24 hours.

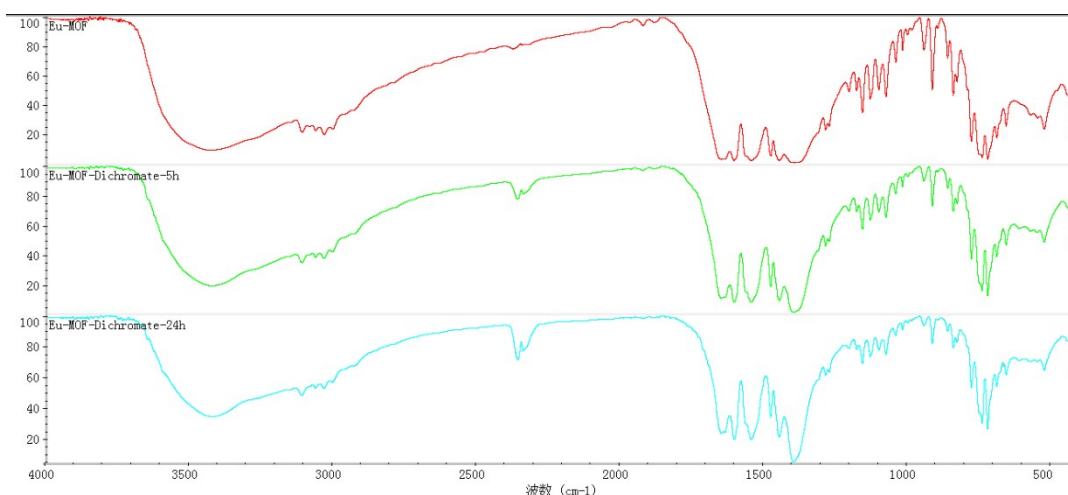


Figure S6. The IR diagrams of Eu-MOF before and after immersing in $\text{Cr}_2\text{O}_7^{2-}$ aqueous solution for 5 hours and 24 hours.

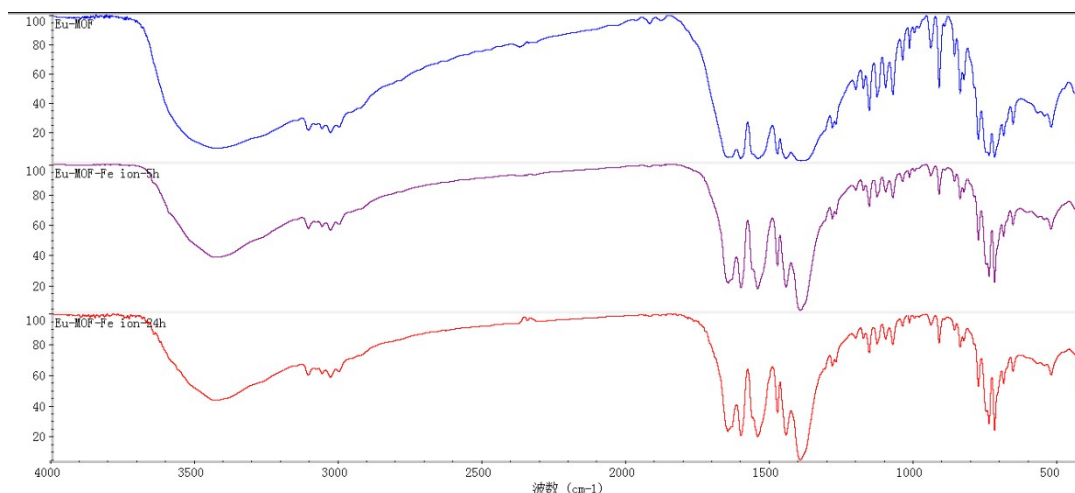


Figure S7. The IR diagrams of Eu-MOF before and after immersing in Fe^{3+} aqueous solution for 5 hours and 24 hours.

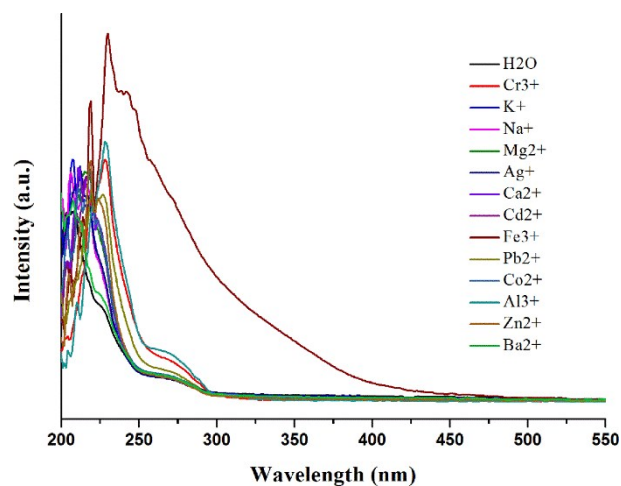


Figure S8. The UV-vis absorption spectra of different cations (0.15mM) in water solution.

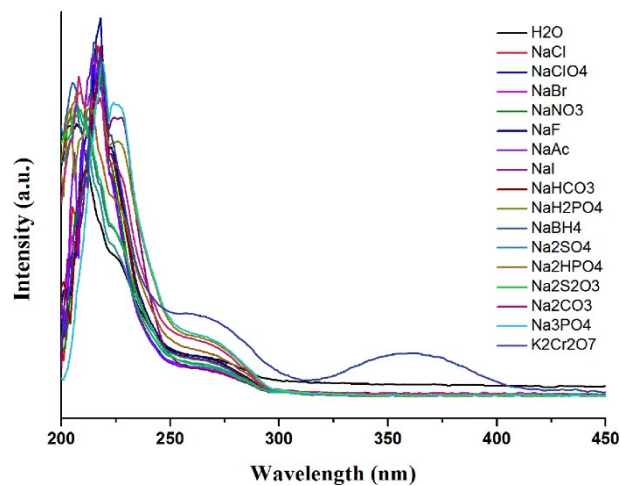


Figure S9. The UV-vis absorption spectra of different anions (0.15mM) in water solution.

References

- [1] J. K. Sun, P. Wang, C. Chen, X. J. Zhou, L. M. Wu, Y. F. Zhang, J. Zhang, Dalton Trans. 41 (2012) 13441.